

The hemodynamic destruction of intravascular cancer cells in relation to myocardial metastasis

(destruction of cancer cells/microcirculation/myocardium)

L. WEISS*, D. S. DIMITROV†, AND M. ANGELOVA†

*Department of Experimental Pathology, Roswell Park Memorial Institute, New York State Department of Health, Buffalo, NY 14263; and †Central Laboratory of Biophysics, Bulgarian Academy of Sciences, 1113 Sofia, Bulgaria

Communicated by David Harker, April 5, 1985

ABSTRACT A variety of observations in humans and experimental animals indicate that large numbers of circulating cancer cells are killed in the microvasculature. It is suggested that this occurs when friction or adhesion between individual cancer cells and capillary walls results in an increase of tension in the cancer cell peripheries above a critical level because of (blood) pressure differentials between their free ends. Hemodynamic and anatomic data relating to the myocardial circulation and deformability measurements on four types of rat cancer cells have been reported previously by others. Novel calculations based on these data suggest that the increased tension at the peripheries of cancer cells passing through the myocardial capillaries will exceed the critical levels for rupture. Analysis of autopsy data for solid tumors reveals a low (<3%) incidence of myocardial metastases in the absence of lung metastases and a higher (15%) incidence in their presence. One explanation for these observations is that, in the absence of lung metastases, relatively few of the cancer cells enter the coronary arteries from primary tumors with systemic venous drainage because many are retained or destroyed in transit through the pulmonary vasculature, and most of those delivered to the myocardium then suffer hemodynamic destruction. In the presence of pulmonary metastases, large numbers of viable cancer cells are liberated directly into the pulmonary venules and subsequently are delivered to the myocardium without prior exposure to the arterial side of the microcirculation. The combined effects of increased delivery and the protective effects of arrested cells on those preceding them in files along the capillaries account for the higher incidence of myocardial metastases. It is proposed that hemodynamic destruction of circulating cancer cells may be an important underlying cause of metastatic inefficiency, together with other cytotoxic mechanisms.

Metastasis and patterns of metastasis are major considerations in the diagnosis and treatment of patients with cancer. In this communication, certain aspects of the development of metastatic patterns will be discussed against the background of mechanical damage inflicted on cancer cells in their transit through the microvasculature.

Cancer cells delivered to organs in their arterial blood fall into three groups: (i) some pass through the vasculature and emerge in the venous blood in the viable state; (ii) other cancer cells are arrested in the microvasculature, and of these comparatively few survive to give rise to metastases; and (iii) many are gradually released with loss of reproductive integrity. The proportions of circulating cancer cells falling into each of the three groups varies with the type of cancer cell and involved organ. For example, in the rat, 98% of AH100B hepatoma cells were killed by one transit of the pulmonary vasculature, compared with only 8% of AH66F hepatoma

cells (1). Other quantitative studies revealed that most W256 cancer cells injected into the tail-veins of rats were arrested in their lungs; but of 5×10^6 cells injected, a mean of <100 lung tumors per animal developed. Most of the arrested cells were gradually released in a nonviable state, and extrapulmonary tumors were therefore infrequent (2). Thus, in common with early histological observations on humans, in which intravascular cancer emboli were seen to contain dead and degenerating cancer cells (3), recent quantitative studies in rodents of the "traffic" of cancer cells also reveal that many cancer cells are destroyed in the microcirculation. This intravascular destruction is considered to be a major factor contributing to "metastatic inefficiency" (4).

The actual mechanisms of intravascular destruction are usually attributed to a variety of cellular and humoral components of the host defense systems; however, it was recently suggested that mechanical trauma inflicted on cancer cells during their passage through the pulmonary microvasculature could also be a major cause of cell loss (5).

In this paper, we wish to examine some of the quantitative and qualitative aspects of mechanical trauma on cancer cells passing through myocardial capillaries in order to assess the feasibility of this mechanism in accounting for the development of metastases in heart muscle.

The Incidence of Metastases in the Myocardium

In the past, metastases to the heart were generally considered to be uncommon, with an overall incidence of 1.5-3% (6-8). This low incidence may well have reflected the short survival of patients with cancer with consequent limitations of the development of metastases in general and/or be due to, as suggested by Willis (9), inadequate autopsy techniques.

As shown in Table 1, the incidence of metastases in the heart (excluding the pericardium) has been reported more recently to lie between 7% and 26%, with a total of 288 of 1934 autopsies (14.9%) performed on people dying as a consequence of "solid" tumors and 290 of 1073 (27%) autopsies in those with lymphoreticular tumors. In the absence of metastases elsewhere, myocardial metastases are rare; in the majority of reported cases, they were associated with intrathoracic metastases. For example, autopsies performed at Roswell Park Memorial Institute from 1959 through 1982 on 9501 patients with malignancies other than primary lung cancer revealed 823 metastases to the heart in 4330 patients with lung metastases (incidence 19%); however, of 5109 patients without lung metastases, only 140 (2.7%) had metastases to the heart (Y. Tsukada and W. W. Lane, personal communication).

Cancer cells are liberated from tumors into the venous blood in very large numbers in humans (18-21) and animals (22-24), and some of them will leave the lungs in the pulmonary veins to be generally disseminated via the aortic blood. Although viable cancer cells leaving the left ventricle usually represent a small proportion of those leaving primary

The publication costs of this article were defrayed in part by page charge payment. This article must therefore be hereby marked "advertisement" in accordance with 18 U.S.C. §1734 solely to indicate this fact.

Table 1. Incidence of heart metastases

Autopsies, no.	Cases with cardiac metastases	% frequency	Ref.
	Solid tumors		
159	28	17.6	(10)
525	66	12.6	(11)
270	20	7.4	(12)
304	37	12.2	(13)
364	55	15.1	(14)
312	82	26.2	(15)
1934 total	288 total	14.9 avg.	
	Lymphoreticular tumors		
43	15	35	(16)
129	25	19.4	(10)
169	61	36.1	(11)
49	19	38.8	(12)
178	69	38.8	(13)
234	60	25.6	(14)
60	9	15.0	(15)
211	32	15.2	(17)
1703 total	290 total	27.0 avg.	

Most of the metastases were present in the myocardium, comparatively few were epicardial or endocardial, and none were pericardial.

tumors, their actual numbers are nonetheless expected to be considerable. Taking human cardiac output as 4.6 liters per min and coronary artery blood-flow as 200–800 ml per min (25), ≈ 4 –17% of the cardiac output is delivered to the myocardium, which therefore may receive appreciable numbers of viable cancer cells. In this context, an attempt will be made to account for the low (<3%) incidence of myocardial metastases in patients with “solid” tumors but without lung metastases and the higher incidence ($\approx 15\%$) in the group with lung metastases.

The Model

In our grossly simplified model of a cancer cell carried by the bloodstream in a capillary, as shown in Fig. 1, the cell is represented by a cylinder with hemispherical ends; the internal contents are assumed to be sufficiently viscous to prevent external fluid stress from being transmitted to the interior of the cell (26, 27). The capillary is represented by a straight tube. The movement of the cell along the tube is facilitated by a lubricating film of plasma between them, the thickness of which is very much smaller than the cell radius. However, because of elastic restoring forces, the cell will tend to expand against the capillary wall and drive out the intervening fluid, with increasing resistance to cell movement along the vessel, until a final equilibrium state of adhesion occurs between them. As the friction increases, the pressure drop between the ends of the cell due to blood pressure will increase, resulting in increased membrane tension, ΔT , over the equilibrium tension, T_e . When $T_e + \Delta T$ exceeds a critical value, the membrane will rupture. In a previous paper (5), a fluid mechanical analysis was developed for the model, with appropriate experimentally determined numerical values for the lung capillaries, plasma, and cells. Cell deformability data for four types of rat cancer cells and the proportions of these cells killed by single intravascular pulmonary transit were reported by Sato and Suzuki (1). Calculations based on these data indicated a critical value for $T_e + \Delta T$ of $5.5 \text{ dyne}\cdot\text{cm}^{-1}$ (1 dyne = 1×10^{-5} N), since this corresponded to the observed death of 98% of AH100B hepatoma cells on one pulmonary transit, whereas lower calculated values were associated with smaller proportions of cell death in other types of hepatoma cells (Table 2).

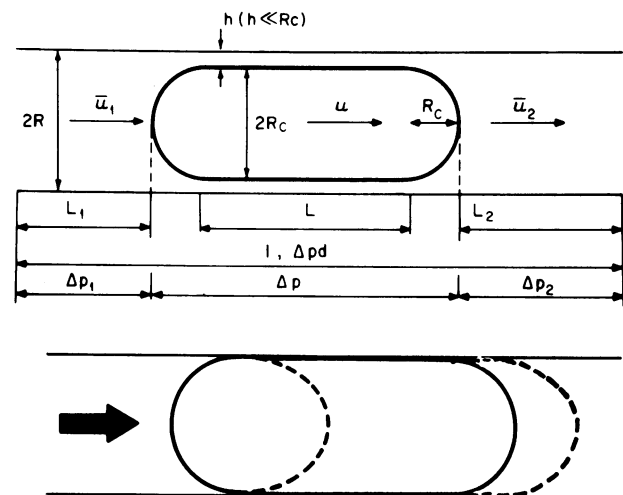


FIG. 1. (Upper) Model of a cancer cell as a cylinder with hemispherical ends, in a capillary of length l . (Lower) Cellular deformation produced (----) by blood pressure (→).

In the present study, the same basic model will be used with numerical values appropriate to the myocardial circulation together with the same cell deformability data of Sato and Suzuki, since the latter cover a wide-range of values.

Myocardial Capillaries and Hemodynamics

In man, capillary diameters range from $4.4 \mu\text{m}$ in systole to $5.2 \mu\text{m}$ in diastole. The actual blood flow in the myocardium is greatly reduced during systole by compressive forces within the myocardium. The cross-sectional area of coronary resistance vessels is also changed by metabolic, neural, and humoral factors intrinsic to the vascular bed (28). In the following calculations, a value of $2.6 \times 10^{-4} \text{ cm}$ will be used for capillary radius (R). Because of the complexity of myocardial vascular anastomoses (29), it is only possible to give approximate values for the length of individual capillary segments; however, 0.1 cm appears to be a reasonable average value.

Reported erythrocyte velocities within the myocardial capillaries of the dog range from $0.2 \text{ cm}\cdot\text{sec}^{-1}$ in systole to $0.15 \text{ cm}\cdot\text{sec}^{-1}$ in diastole (30), and a range of 0.1 to $0.2 \text{ cm}\cdot\text{sec}^{-1}$ appears generally acceptable for diastole in humans.

In the rat, blood pressure values of 67 and 45 mm of Hg (1 mm of Hg = 133.3 Pa) have been recorded in systole and

Table 2. Calculated values at cancer cell peripheries

Cancer cell type	T_e^*	Pulmonary $T_e + \Delta T^\dagger$	Cells killed by one	
			pulmonary transit (1), %	Myocardial $T_e + \Delta T^\ddagger$
AH100B	3.9	5.5	98	11.2
AH130	2.6	4.2	59	9.9
AH66F	0.9	2.5	8	8.2
YS	0.9	2.5	8	8.2

Equilibrium tensions (T_e) from ref. 5, blood pressure-induced increases in tension (ΔT), and total tension ($T_e + \Delta T$) in the peripheries of the specified cancer cell types in pulmonary and myocardial capillaries, under the condition $K = 0$, are all in $\text{dyne}\cdot\text{cm}^{-1}$.

*Values calculated from cell deformability measurements (1).

†Total tension at cancer cell peripheries in pulmonary microcirculation from ref. 5.

‡Total tension at cancer cell peripheries in myocardial microcirculation.

diastole respectively, in the small (0.0025- to 0.01-cm diameter) coronary arterioles; in the small coronary venules (0.005- to 0.01-cm diameter), corresponding values were 24 and 5 mm of Hg (30). Therefore, we have taken a mean value of 42 mm of Hg ($56 \times 10^3 \text{ dyne}\cdot\text{cm}^{-2}$; $1 \text{ dyne}\cdot\text{cm}^{-2} = 0.1 \text{ Pa}$) for the pressure drop along the interposed capillaries. In the rat, average aortic blood pressures were 100 (systolic) and 70 (diastolic) mm of Hg, respectively; therefore, the other given values appear to be appropriate to humans.

Calculations of Blood-Pressure-Induced Cell-Membrane Damage

Blood-pressure-induced increases in membrane tension (ΔT) are given by (5):

$$\Delta T = \frac{\Delta p \cdot R_c}{2},$$

where Δp is the pressure drop in $\text{dyne}\cdot\text{cm}^{-2}$ between the ends of a cancer cell, and R_c is the cell radius, which closely approximates to capillary radius R ($2.6 \times 10^{-4} \text{ cm}$) as shown in Fig. 1.

The relationship between the pressure drop between the ends of a cancer cell (Δp) and the pressure drop or driving pressure, Δp_d , between the ends of a capillary segment is given by

$$\Delta p = \frac{1}{1 + K} \cdot \Delta p_d \text{ (see Appendix).}$$

The more closely a cell is applied to a capillary wall, the more will the pressure drop between its ends approximate to the driving pressure along the capillary segment. Therefore, as K is proportional to the separation between the two surfaces, the lower the value of K , the more likely is membrane rupture due to hemodynamic forces. In the situation where a cancer cell is adherent to and blocking a capillary (i.e., $K = 0$), the pressure drop between the ends of the cell will be maximal and equal to the driving pressure along the capillary segment. Under these conditions in a myocardial capillary, ΔT has a calculated value of $7.3 \text{ dyne}\cdot\text{cm}^{-1}$, compared with the value $1.6 \text{ dyne}\cdot\text{cm}^{-1}$ previously obtained for cancer cells within the pulmonary capillaries. In the latter situation, as shown in Table 2, when the sum of the calculated equilibrium tension T_e and ΔT attained a value of $5.5 \text{ dyne}\cdot\text{cm}^{-1}$, 98% of AH100B cancer cells were killed by one pulmonary passage in the rat, and lower values corresponded to less killing.

The present summated values of tensions for the same four cancer cell types within the myocardial capillaries exceed the highest value previously obtained for the pulmonary microcirculation under comparable conditions (5) and, therefore, indicate that more intravascular cancer cell death is expected in the myocardium than in the lungs.

As shown in the Appendix, possible values for K range from 0.4 to 38; however, as discussed below, consideration of film thickness in relation to transit times makes the lower value more probable. By using this value for K (0.4), the calculated tensions ($T_e + \Delta T$) in the myocardial microcirculation for the AH100B, AH130, AH66F, and YS cells are 9.1, 7.8, 6.1, and $6.1 \text{ dyne}\cdot\text{cm}^{-1}$, respectively.

Cancer Cell Arrest in Relation to Transit Time

To form metastases, cancer cells must first be arrested in the myocardial microvasculature. However, adhesion of cancer cells to vessel walls is delayed by the presence of interposed films of plasma, which must be reduced to a critical final thickness, h_f , to permit interactions leading to adhesion. It is assumed that when adhesion occurs, there is a zero contact angle between the cell membrane and the vessel wall. Therefore, the probability of adhesion depends on the time

taken for the necessary reduction in film thickness in relation to the time taken for cells to pass completely along capillary segments. This can be approached in a semiquantitative manner on the basis of the approaches outlined elsewhere (5, 31, 32).

The velocity, u , of whole cancer cells is given by (5):

$$u = \Delta p \cdot h \cdot R / 2 \cdot \mu \cdot L,$$

where h is the average lubricating film thickness, which is expected to be $\approx 10^{-6} \text{ cm}$; R , the capillary radius, is $2.6 \times 10^{-4} \text{ cm}$; μ , the plasma viscosity, is $\approx 2 \times 10^{-2}$ poise ($1 \text{ poise} = 0.1 \text{ Pa}\cdot\text{sec}$); and L , the length of the cell opposed to the vessel wall, is $\approx 4 \times 10^{-3} \text{ cm}$.

Under these conditions, the calculated velocity of $\approx 0.1 \text{ cm}\cdot\text{sec}^{-1}$, which corresponds to a transit time of 1 sec in a capillary of 0.1-cm length, is lower but of the same order of magnitude as velocities reported for erythrocytes by Tillmanns *et al.* (30) and others. However, as the cancer cells have mean diameters ranging from 12 to $15.3 \mu\text{m}$ (1), compared with $\approx 7 \mu\text{m}$ for erythrocytes, it is expected that their velocities in the capillaries would be lower.

Adhesion time, τ_a , is given by (5):

$$\tau_a = \frac{\mu \cdot R \cdot L^2}{2Th_f^2}.$$

Values for membrane tension, T , must lie between equilibrium tension (T_e) and $T_e + \Delta T$ as given in Table 2. In Fig. 2, calculations of τ_a with respect to h_f are shown for a range of values for T , appropriate for cancer cells at equilibrium and in the myocardial and pulmonary capillaries.

The results indicate adhesion times in excess of transit times for all values of membrane tension when h_f is less than $\approx 20 \text{ nm}$ but indicate that transit times would be long enough for adhesion to occur at higher values of h_f . In terms of h_f -regulated adhesion, the results indicate that, for the four types of cancer cells, arrest in the myocardial capillaries is more probable than in those of the lungs. These comparisons are made between cancer cells delivered to the myocardium via the left ventricle and to the pulmonary microcirculation via the right ventricle. An index of the trapping efficiency of the myocardial vasculature is provided by the ratio of vascularity (i.e., cell input) to arrest of cancer cells. Vascularity may be expressed as the percentage of cardiac output going to an organ and may be determined by measurement of the arrest of radiolabeled microspheres after left ventricular injection (33). In mice, 2 min after left-ventricular injection of ^{125}I -labeled carbonized-plastic $15\text{-}\mu\text{m}$ diameter microspheres, 4.7% of the dose was detected in the myocardium compared with the arrest of 5% of the total dose of radiolabeled B16 melanoma cells 5 min after left-ventricular injection (34). The ratio of vascularity to cell trapping for the myocardium is therefore 0.94. In mice, 5 min after tail vein injections, which correspond to right-ventricular injections, between 70% and 90% of four different types of mouse cancer cells were arrested in the lungs (35). Thus, the experimental evidence is in general accord with the calculations shown in Fig. 2, suggesting that a greater proportion of cancer cell input is trapped in the myocardium than in the lungs.

In the early stages of extrathoracic cancer, very often the only cancer cells delivered to the myocardium are those surviving transit through the pulmonary circulation. However, the proportional arrest data for these two organs is not expected to correlate with a higher incidence of myocardial metastasis because greater absolute numbers of viable cancer cells will be arrested in the lungs, which are the first organs encountered, than in the myocardium. In addition, of those cells delivered, greater proportions are expected to be destroyed in the myocardium than in the lungs.

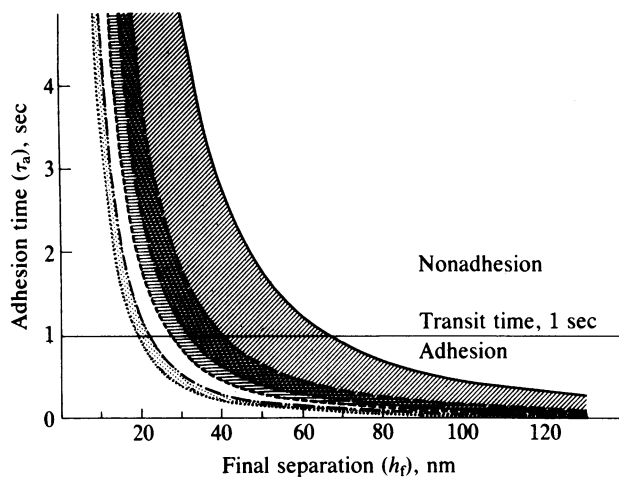


FIG. 2. Dependence of adhesion time (τ_a) on final lubricating film thickness h_f for tensions within the range calculated for AH100B (high) and YS (low) cancer cells under the conditions shown in Table 2. ▨, Range within the myocardial capillaries; ▩, range within pulmonary capillaries; ▤, equilibrium tensions; ▥, overlap. Adhesion to the capillary walls is expected when, within transit time, h_f is reduced to values permitting the adhesive process to be initiated.

Conclusions: Hemodynamic Damage and Patterns of Myocardial Metastasis

As with all models, our own is oversimplified; in focusing on the surface membranes, we have studiously ignored the effects of internal structures, particularly the nucleus and cytoskeleton. We have assumed that various stresses are supported exclusively by a smooth cell surface membrane surrounding a homogeneous interior with no stress gradients. There is the very real possibility that membrane rupture could be due to a localization of stresses, as distinct from the uniform traction discussed here. However, while detailed analyses indicate that the viscoelastic behavior of normally extended leukocytes is primarily due to their cytoplasm (36), once their membranes are stretched taut as is presumed in the present case of cancer cells, the membrane stresses may be considerable. We are concerned here exclusively with membrane rupture in cancer cells.

An additional factor to be considered is the effect of membrane ruffling because, in its presence, cell extension could take place by unfolding, without increase in membrane tension. In the case of leukocytes, the ruffles may approximately double their true surface areas compared with spheres of equivalent volumes (37-39). Thus, ruffling would have a protective effect in tension-induced trauma and, together with their relatively small diameter and low nuclear/cytoplasmic ratio, may indeed serve to protect circulating leukocytes from mechanical damage. However, as far as we are aware, the relative susceptibilities to trauma of the cells listed in Table 2 are not overtly related to surface ruffling, and it is noteworthy that even if there were only a 5% surface expansion due to stretching, as distinct from unruffling, then rupture would be expected (25). Thus, ruffling of surface membranes appears to be more important in leukocytes, which are *not* killed in the microcirculation, than in cancer cells, which are.

When comparatively small numbers of cancer cells enter the coronary arteries, at any one time only single cancer cells will be present in individual capillary segments. Under these conditions, our calculations indicate that pressure-induced cell destruction is likely to occur to a considerable extent. Because of current uncertainties in ascribing values to the final separation between the cancer cell peripheries and the microvascular walls (h_f), it is impossible to unequivocally

calculate the likelihood of cancer cell arrest in the ventricular microcirculation. However, from the viewpoint of metastasis, this is noncritical because, on the one hand, if single cancer cells are not arrested, they cannot form metastases; but on the other hand, if they are arrested, they will tend to be destroyed by pressure differentials.

Thus, in the presence of small numbers of circulating cancer cells, intravascular destruction is expected to account for the low (<3%) incidence of hematogenous, myocardial metastases observed in people dying as a consequence of early solid tumors.

The situation is expected to be different when sufficiently large numbers of cancer cells enter the coronary arteries to give rise to files of cancer cells in individual capillary segments. In this case, if one cell in a file were arrested, causing a block of blood-flow in that particular segment, the cells preceding it would no longer be subject to a pressure-differential and, thus, would be protected from this type of intravascular destruction. The arrested cell would be destroyed and the preceding cells would cease moving and, subject to other constraints, would have the potential to form metastases. Arrest would be facilitated in cancer cells of larger than average size or tension, but survival from mechanical trauma is not a heritable property of subpopulations (40).

In view of the cancer cell-trapping and -killing capacity of the pulmonary microcirculation, relatively few of the cancer cells leaving a primary tumor are expected to survive passage through the lungs. In the case of cancer cells leaving primary tumors with main venous drainage into the portal system [e.g., adenocarcinomas of the upper rectum (41)], even fewer cells are expected to survive passage through both the hepatic and pulmonary microvasculature. Therefore, it is considered that the commonest way in which large numbers of viable cancer cells can enter the coronary arteries is from lung tumors (primary or metastatic lesions) via the pulmonary veins. Under these circumstances, the incidence of myocardial metastases is in fact comparable to that in many other organs (41).

The fact that, of patients dying with pulmonary metastases, $\approx 80\%$ do not have myocardial metastases may indicate that the myocardial microcirculation can effectively kill large numbers of cancer cells and that death occurred from other causes before this hemodynamic protective mechanism was overwhelmed.

The dose-dependant mechanism of metastasis development proposed here may explain the sequence of development of patterns by metastasis as described in semiquantitative terms by Viadana *et al.* (42). In addition, in demonstrating differences between the extent of hemodynamic damage to cancer cells in the microcirculation of at least two organs, the lungs and heart, our calculations possibly indicate a novel basis for differential organ hostility, which also may influence the formation of metastatic patterns. The generality of fluid mechanical damage suggests that it may make significant contributions to the phenomenon of metastatic inefficiency. Although we have emphasized the role of increased tension in causing membrane rupture and cancer cell death, other more subtle and sublethal forms of mechanical damage may occur (43). Additional mechanically induced trauma is expected during entry of cancer cells into the capillaries.

During systole, the myocardial microvasculature is virtually closed down by contraction of the cardiac muscle. Compression of the intraluminal cells tends to lead to their expulsion or, if they remain because of adhesion to the vessel walls, considerable increases in their membrane tension. This could lead to even more intravascular trauma than calculated on the basis of blood-pressure differentials alone. However, at present, this effect cannot be enumerated.

In addition to the cancer cells, the microvascular endothelial cells also will be subject to frictional forces and damage, which is known to trigger a wide spectrum of events linking inflammatory and coagulation processes (35). Some of these cause cancer cell injury and death, whereas some facilitate intravasation/invasion. When reactive expansion of cancer cells occurs, concurrent nontraumatic expansion of the opposing vessel wall would tend to inhibit the displacement of the intervening (lubricant) fluid and, thereby, inhibit cancer cell damage. The extent of vessel expansion will be limited by the basement membrane surrounding the vessel and by the compliance of the supporting tissues (44). Intuitively, more expansion would be expected in the pulmonary microvasculature with relatively sparse and elastic supporting alveolar tissues, than in the densely supported myocardial vasculature.

Finally, the proposed mechanisms are not considered to be unique in causing the intravascular death of cancer cells during metastasis.

APPENDIX

In the system shown schematically in Fig. 1, the flow of fluid between the cell and the capillary wall will be negligible when the thickness, h , of the lubricating liquid film is much smaller than the radius, R_c , of the deformed cell.

Cell velocity, u , will be equal to the average of the velocities of the fluid behind (\bar{u}_1) and ahead (\bar{u}_2) of the cell and is given by (5):

$$u = \frac{hR}{2\mu L} \cdot \Delta p,$$

where μ is the viscosity of the fluid.

Under the above conditions,

$$\Delta p_d = \Delta p_1 + \Delta p + \Delta p_2,$$

$$u = \bar{u}_1 = \bar{u}_2.$$

The Poiseuille equation gives

$$\bar{u}_1 = \frac{R^2}{8\mu L_1} \cdot \Delta p_1,$$

$$\bar{u}_2 = \frac{R^2}{8\mu L_2} \cdot \Delta p_2.$$

By solving the equations with respect to Δp ,

$$\Delta p = \frac{1}{1 + K} \cdot \Delta p_d,$$

where

$$K = \frac{4 h L_0}{RL},$$

$$L_0 = L_1 + L_2 = l - (L + 2R_c),$$

and l is the length of the capillary segment.

By ascribing the following numerical values:

$$R = 2.6 \times 10^{-4} \text{ cm } (R_c \approx R),$$

$$l = 0.1 \text{ cm},$$

$$L = 40 \times 10^{-4} \text{ cm } (L_0 = 0.1 \text{ cm}),$$

$$h = 0.01 \times 10^{-4} \text{ to } 1 \times 10^{-4} \text{ cm},$$

the parameter K varies from 0.37 to 37, depending on the value of h .

The work reported here was initiated during a Bulgarian Academy of Sciences/U.S. National Academy of Sciences exchange visit (L.W.) and has been continued with the partial support of the American Cancer Society (Grants CD-21 and PDT-273), the Bulgarian Academy of Sciences, and the State Committee for Science and Technology of the Peoples Republic of Bulgaria.

1. Sato, H. & Suzuki, M. (1972) in *Fundamental Aspects of Metastasis*, ed. Weiss, L. (North-Holland, Amsterdam), pp. 311–317.
2. Weiss, L. (1980) *Int. J. Cancer* **25**, 385–392.
3. Iwasaki, T. (1915) *J. Pathol. Bact.* **20**, 85–105.
4. Weiss, L. (1982) in *Liver Metastasis*, eds. Weiss, L. & Gilbert, H. A. (Hall, Boston), pp. 126–157.
5. Weiss, L. & Dimitrov, D. S. (1984) *Cell Biophys.* **6**, 9–22.
6. Pic, A. & Bret, J. (1891) *Rev. Med.* **11**, 1022–1041.
7. Symmers, D. (1917) *Am. J. Med. Sci.* **154**, 225–240.
8. Pollia, J. A. & Gogol, L. J. (1936) *Am. J. Cancer* **27**, 229–233.
9. Willis, R. A. (1952) *The Spread of Tumors in the Human Body* (Butterworth, London), p. 150.
10. Burnett, R. C. & Shimkin, M. B. (1954) *Arch. Intern. Med.* **93**, 205–218.
11. Hanfling, S. M. (1960) *Circulation* **22**, 474–483.
12. Malaret, G. E. & Aliaga, P. (1968) *Cancer* **22**, 457–466.
13. Bisel, H. F. & LaDue, J. S. (1953) *J. Am. Med. Assoc.* **153**, 712–715.
14. DeLoach, J. F. & Haynes, J. W. (1953) *Arch. Intern. Med.* **91**, 224–249.
15. Young, J. M. & Goldman, I. R. (1954) *Circulation* **9**, 222–229.
16. Kirshbaum, J. D. & Preuss, F. S. (1943) *Arch. Intern. Med.* **71**, 777–792.
17. Madianos, M. & Sokal, J. E. (1963) *Am. Heart J.* **65**, 322–326.
18. Griffiths, J. D. & Salsbury, A. J. (1965) *Circulating Cancer Cells* (Thomas, Springfield, IL).
19. Malmgren, R. A. (1968) *Twenty-first Symposium on Fundamental Cancer Research* (Williams and Wilkins, Baltimore, MD), pp. 481–494.
20. Nadel, E. M., ed (1965) *Acta Cytol.* **9**, 3–188.
21. Koo, J., Fung, K., Siu, K. F., Lee, N. W., Lett, Z., Ho, J., Wong, J. & Ong, G. B. (1983) *Cancer* **52**, 1952–1956.
22. Glaves, D. (1983) *Br. J. Cancer* **48**, 665–673.
23. Glaves, D. & Mayhew, E. (1984) *Cancer Drug Deliv.* **1**, 293–302.
24. Mayhew, E. & Glaves, D. (1984) *Br. J. Cancer* **50**, 159–166.
25. Burton, A. C. (1972) in *Physiology and Biophysics of the Circulation* (Year Book Medical, Chicago, IL), 2nd. Ed. pp. 88–91.
26. Goldsmith, H. L. & Mason, S. G. (1962) *J. Fluid Mech.* **14**, 42–58.
27. Goldsmith, H. L. & Mason, S. G. (1963) *J. Colloid Interface Sci.* **18**, 237–261.
28. Braunwald, E. & Sobel, B. E. (1980) in *Heart Disease*, ed. Braunwald, E. (Saunders, Philadelphia), pp. 1279–1305.
29. Berne, R. M. & Rubio, R. (1979) in *Handbook of Physiology, The Heart* ed. Berne, R. M. (Am. Physiol. Soc., Bethesda, MD), Vol. 1, pp. 873–952.
30. Tillmanns, H., Ikeda, S., Hansen, H., Sorma, J. S., Fauvel, J. M. & Bing, R. J. (1974) *Circ. Res.* **34**, 561–569.
31. Dimitrov, D. S. (1983) *Prog. Surf. Sci.* **14**, 295–423.
32. Dimitrov, D. S. & Jain, R. K. (1984) *Biochim. Biophys. Acta* **779**, 437–468.
33. Heymann, M. A., Payne, B. D., Hoffman, J. I. E. & Rudolph, A. M. (1977) *Prog. Cardiovasc. Res.* **20**, 55–79.
34. Weiss, L., Ward, P. M., Harlos, J. P. & Holmes, J. P. (1984) *Int. J. Cancer* **33**, 825–830.
35. Weiss, L. & Glaves, D. (1983) *Ann. N. Y. Acad. Sci.* **416**, 681–692.
36. Skalak, R., Chien, S. & Schmid-Schönbein, G. (1984) in *White Cell Mechanics: Basic Science and Clinical Aspects*, eds. Meiselman, H. S., Lichtman, M. A. & LaCelle, P. L. (Liss, New York), pp. 3–18.
37. Bagge, U. (1976) *Blood Cells* **2**, 481–490.
38. Schmid-Schönbein, G. W., Sung, K. L. P., Tozeren, H., Skalak, R. & Chien, S. (1981) *Biophys. J.* **36**, 243–256.
39. Evans, E. A. (1984) in *White Cell Mechanics: Basic Science and Clinical Aspects*, eds. Meiselman, H. J., Lichtman, M. A. & LaCelle, P. L. (Liss, New York), pp. 53–71.
40. Gabor, H. & Weiss, L. (1985) *Invasion Metast.* **5**, 71–83.
41. Weiss, L., Voit, A. & Lane, W. W. (1984) *Invasion Metast.* **4**, 47–60.
42. Viadana, E., Bross, I. D. J. & Pickren, J. W. (1978) in *Pulmonary Metastasis*, eds. Weiss, L. & Gilbert, H. A. (Hall, Boston, MA), pp. 143–167.
43. Gabor, H. & Weiss, L. (1985) *Invasion Metast.* **5**, 84–95.
44. Fung, Y. C. (1981) *Biomechanics: Mechanical Properties of Living Tissues* (Springer, New York), pp. 286–290.
45. Tillmanns, H., Steinhausen, M., Leinberger, H., Thederan, H. & Kübler, W. (1981) *Circ. Res.* **49**, 1202–1211.